Neuron, Vol. 42, 653–663, May 27, 2004, Copyright ©2004 by Cell Press

Heterosynaptic Dopamine Neurotransmission Selects Sets of Corticostriatal Terminals

Nigel S. Bamford,[1,2] Hui Zhang,[2] Yvonne Schmitz,[2] Nan-Ping Wu,[5] Carlos Cepeda,[5] Michael S. Levine,[5] Claudia Schmauss,[3,6] Stanislav S. Zakharenko,[4] Leonard Zablow,[4] and David Sulzer[2,3,6,*]

[1]Department of Neurology
Department of Pediatrics
University of Washington
Children's Hospital and Regional Medical Center
Seattle, Washington 98105
[2]Department of Neurology
[3]Department of Psychiatry
[4]Center for Neurobiology and Behavior
Howard Hughes Medical Institute
Columbia University College of Physicians and Surgeons
New York, New York 10032
[5]Mental Retardation Research Center
The David Geffen School of Medicine
University of California at Los Angeles
Los Angeles, California 90095
[6]Department of Neuroscience
New York State Psychiatric Institute
New York, New York 10032

Summary

Dopamine input to the striatum is required for voluntary motor movement, behavioral reinforcement, and responses to drugs of abuse. It is speculated that these functions are dependent on either excitatory or inhibitory modulation of corticostriatal synapses onto medium spiny neurons (MSNs). While dopamine modulates MSN excitability, a direct presynaptic effect on the corticostriatal input has not been clearly demonstrated. We combined optical monitoring of synaptic vesicle exocytosis from motor area corticostriatal afferents and electrochemical recordings of striatal dopamine release to directly measure effects of dopamine at the level of individual presynaptic terminals. Dopamine released by either electrical stimulation or amphetamine acted via D2 receptors to inhibit the activity of subsets of corticostriatal terminals. Optical and electrophysiological data suggest that heterosynaptic inhibition was enhanced by higher frequency stimulation and was selective for the least active terminals. Thus, dopamine, by filtering less active inputs, appears to reinforce specific sets of corticostriatal synaptic connections.

Introduction

Axon-to-axon communication by modulatory neurotransmitters acting on presynaptic G protein-coupled receptors has long been suggested to provide a major form of central neurotransmission and modulation. A prominent example of such a proposed circuit is suggested for the dopaminergic regulation of voluntary motor learning. The basic "striatal microcircuit" (Figure 1A) consists of corticostriatal glutamatergic projections (Wilson, 1987) that form asymmetric synaptic contacts with the dendrites of medium spiny neurons (MSNs) and nearby nigrostriatal dopaminergic projections from ventral midbrain neurons that form symmetrical synapses on MSN dendrites (Graybiel et al., 1981). This configuration suggests that dopamine release, which is elicited by salient behavioral stimuli that evoke burst firing in ventral midbrain neurons or by dopamine-releasing drugs such as amphetamine, may not only modulate the excitability of MSNs (Nicola et al., 2000) but may also diffuse from the synaptic cleft to activate nearby dopamine receptors on cortical presynaptic terminals (Garris et al., 1994; Gonon, 1997).

The hypothesis that dopamine alters the excitatory input to MSNs generated by the cortex has been evaluated by electrophysiological recordings of MSNs. Despite numerous studies, however, it remains controversial whether dopamine modulates corticostriatal terminal activity. Both excitatory and inhibitory effects by dopamine agonists on MSNs have been reported and interpreted to indicate responses elicited by either D1-like (Harvey and Lacey, 1996; Nicola et al., 1996; Nicola and Malenka, 1998) or D2-like (Calabresi et al., 1993; Cepeda et al., 2001; Flores-Hernandez et al., 1997; Garcia-Munoz et al., 1991; Hsu et al., 1995; Maura et al., 1988; O'Donnell and Grace, 1994; Tang et al., 2001; West and Grace, 2002) receptors. Some studies found no effects unless animals were subjected to interventions designed to drive dopamine receptor signaling into a supersensitive state (Nicola et al., 1996). Indirect evidence suggests that presynaptic D1-like receptors modulate activity of glutamatergic terminals in the ventral (Harvey and Lacey, 1996; Nicola et al., 1996; Nicola and Malenka, 1998) but not dorsal (Nicola and Malenka, 1998) striatum. Although some of the studies above suggest an inhibition of corticostriatal transmission by D2-like receptors, it remains unclear whether these effects are due to pre- or postsynaptic effects on the corticostriatal synapse.

Immunohistochemical analyses of rat motor striatum by electron microscopy have also been controversial, revealing exceedingly rare (Hersch et al., 1995) or low (Fisher et al., 1994; Sesack et al., 1994; Wang and Pickel, 2002) levels of dopamine receptors on corticostriatal terminals. D1 receptors may be exclusively localized on postsynaptic elements (Caille et al., 1996; Hersch et al., 1995; Levey et al., 1993), while D2 receptors may be localized on pre- and postsynaptic elements, including a subpopulation of corticostriatal terminals (Fisher et al., 1994; Hersch et al., 1995; Sesack et al., 1994; Wang and Pickel, 2002). Thus, the action and even presence of dopamine receptors on corticostriatal terminals remain unestablished, although these issues are paramount to understanding striatal function. Here, we introduce an approach to address these questions at the level of individual synaptic terminals and find direct evidence

*Correspondence: ds43@columbia.edu

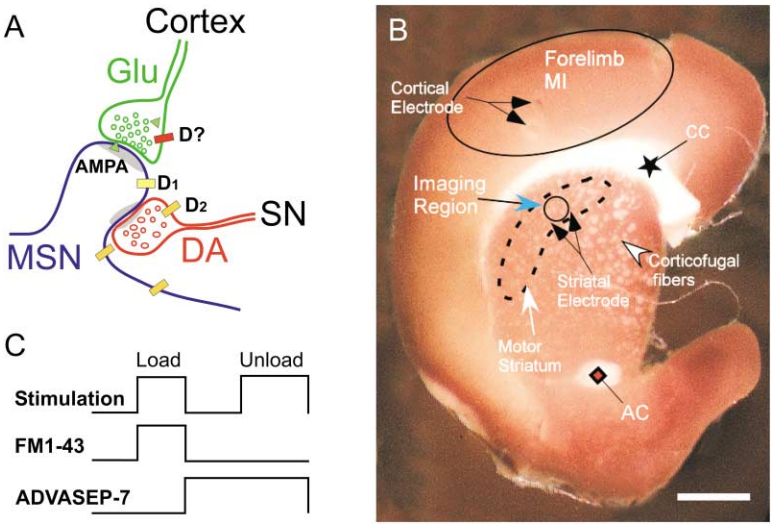

Figure 1. Loading of Corticostriatal Terminals with FM1-43

(A) Cartoon of the basic "striatal microcircuit." GLU, glutamatergic afferent; SN, substantia nigra; MSN, medium spiny neuron; DA, dopamine afferent; AMPA, α-amino-3-hydroxy-5-methyl-4-isoxazolepropionic acid (AMPA) receptor; D, dopamine receptor subtype.

(B) A corticostriatal slice stained with 3,3′-diaminobenzidine shows the areas of stimulation and recording. Corticostriatal terminals from the forelimb primary motor cortex (MI) were loaded with FM1-43 by stimulation with bipolar electrodes placed over cortical layers 5-6 (indentations from the electrodes are visible at the upper arrows). 2-photon images of corticostriatal terminals were obtained from the corresponding forelimb MI motor striatum (circle within the motor striatum). Dopamine was released by local striatal stimulation (striatal electrode). CC, corpus callosum (asterisk); AC, anterior commissure (diamond). Scale bar equals 1 mm.

(C) Protocol for loading and destaining corticostriatal terminals with FM1-43.

that dopamine D2 receptors indeed regulate corticostriatal presynaptic terminal activity. This regulation is in turn dependent on the frequency of stimulation applied to corticostriatal afferents and appears to provide a mechanism to select subsets of corticostriatal input onto MSNs.

Results

Optical Measurements of Presynaptic Activity

In order to more directly observe possible presynaptic actions of dopamine on corticostriatal activity, we directly assessed the activity of individual corticostriatal terminals in the dorsal striatum by combining 2-photon microscopy of FM1-43 fluorescence and amperometric recordings in corticostriatal slices prepared from adult mice. The corticostriatal projection was stimulated using bipolar electrodes placed over layers V-VI (Wilson, 1987) of the motor cortex. Activity of corticostriatal terminals was recorded optically in the motor striatum at a distance of 1.5–2.0 mm from the stimulating electrode (Figures 1B and 1C). Stimulation induced FM1-43 uptake by endocytosis, and subsequent stimuli induced release of this dye during synaptic vesicle exocytosis, providing a measure of presynaptic terminal activity (Betz and Bewick, 1992). Recordings were performed in the presence of glutamate receptor antagonists to inhibit retrograde effects (see Experimental Procedures and following section). Following incubation with the fluorescent quenching agent ADVASEP-7 to remove adventitious staining (Kay et al., 1999), images of striatal terminals loaded by cortical stimulation revealed linear arrays of puncta (diameter = 0.81 ± 0.25 μm, mean ± SEM, n = 81) characteristic of en passant corticostriatal afferents (Wilson, 1987). The puncta in Figure 2A destained with half-times ($t_{1/2}$; the time that fluorescence intensity decayed to half of its initial value) ranging from 170 to 320 s. The data are displayed to indicate destaining starting at a normalized intensity, typically decreasing in a near-exponential fashion to background (~10%), so that the greatest difference between conditions was observed near the middle of the curves (Figure 2B).

Unloading of FM1-43 Is Dependent on Frequency and Calcium and Independent of Postsynaptic Feedback

Stimulated destaining was dependent on the frequency of applied stimulation (Figure 2B), exhibiting a pronounced slope near 10 Hz (Figure 2C), suggesting that this frequency would be sensitive for detecting responses to pharmacological and physiological manipulations. This frequency is consistent with physiological corticostriatal neuron firing rates (Stern et al., 1997). The mean fractional destaining per stimulus (*f*; see Experimental Procedures) at 1 Hz was 0.21% ± 0.02%, similar to previous reports (Isaacson and Hille, 1997). There was a marked frequency-dependent depression of destaining, so that the mean fractional destaining per stimulus declined to f = 0.038% ± 0.005% at 10 Hz, f = 0.013% ± 0.002% at 20 Hz, and f = 0.013% ± 0.003% at 50 Hz ($p < 0.001$, $F = 83.75$, ANOVA).

Stimulated destaining was dependent on Ca^{2+} and was blocked by 200 μM Cd^{2+} (Figure 3A; Zakharenko et al., 2001). An increase in the Ca^{2+}/Mg^{2+} ratio enhanced destaining ($t_{1/2}$ = 176 s for controls versus 139 s for 5 mM Ca^{2+}; $p < 0.001$), whereas a decreased Ca^{2+}/Mg^{2+} ratio slowed destaining ($t_{1/2}$ = 328 s for trace Ca^{2+}; $p < 0.001$; Figures 3B and 3C), consistent with regulated vesicular exocytosis.

We examined a potential role for glutamate-mediated feedback pathways on corticostriatal destaining by loading and destaining striatal terminals with FM1-43 in the presence and absence of the NMDA receptor antagonist D-APV (50 μM), the AMPA receptor antagonist NBQX (10 μM), and the metabotropic glutamate receptor antagonist (*S*)-MCPG (300 μM). The destaining kinetics of D-APV- and NBQX-treated sections ($t_{1/2}$ = 187 s; n = 165 puncta from 7 slices) and (*S*)-MCPG-

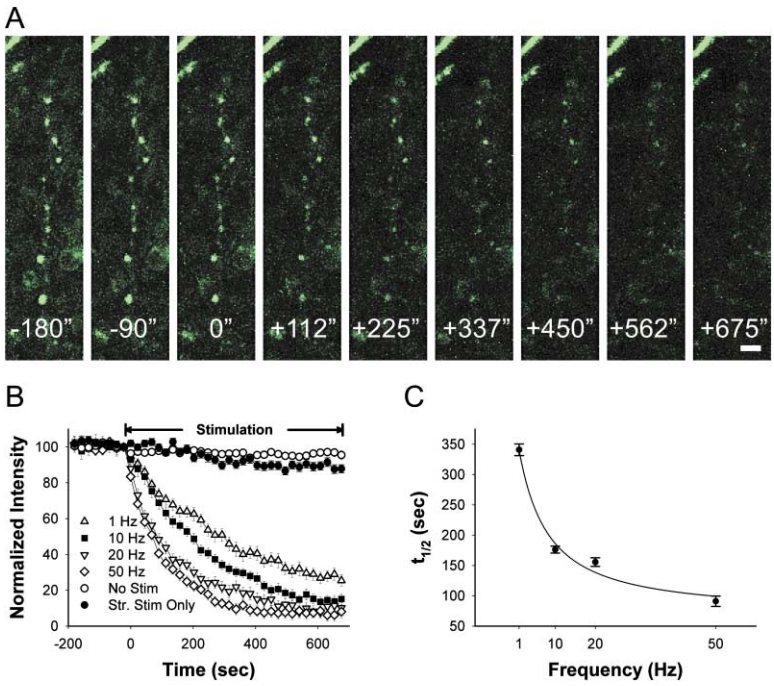

Figure 2. Stimulation and Frequency-Dependent Destaining of FM1-43 from Corticostriatal Terminals

(A) Stimulation of the forelimb motor cortex in the presence of FM1-43 resulted in labeled puncta in en passant arrays. Restimulation of the forelimb motor cortex at 10 Hz (200 μs, 400 μA) resulted in activity-dependent destaining. Stimulation began at t = 0. Scale bar equals 2 μm.

(B) Corticostriatal terminal destaining is frequency dependent, showing differential response to stimulation at 1 Hz (n = 47 puncta from 5 slices), 10 Hz (n = 54 puncta, 8 slices), 20 Hz (n = 62 puncta from 4 slices), and 50 Hz (n = 64 puncta from 7 slices). Controls receiving either no stimulation (n = 116 puncta from 4 slices) or only striatal stimulation at 0.1 Hz (n = 235 puncta from 7 slices) showed minimal destaining. Data points represent mean ± SEM.

(C) The half-time decay of fluorescence intensity ($t_{1/2}$) for 1, 10, 20, and 50 Hz stimuli shows the dependence of destaining on stimulation frequency. The data was fit by the equation $t_{1/2} = t_{1/2}$ (min) + q/f, where $t_{1/2}$ (min) is the minimal half-time at high frequencies, f is the frequency of stimulation (Hz), and q is an arbitrary constant (Zakharenko et al., 2001).

exposed sections ($t_{1/2}$ = 181 s; n = 105 puncta from 4 slices) were similar to controls ($t_{1/2}$ = 176 s; n = 193 puncta from 8 slices; $p > 0.1$), indicating that under our conditions there was no effect on destaining rates due to corticostriatal glutamate release and a consequent feedback pathway. Likewise, in combination with NBQX, the $GABA_B$ antagonist CGP 52432 (10 μM; $t_{1/2}$ = 198 s; n = 142 puncta from 4 slices; $p > 0.5$) and the adenosine A1 antagonist DPCPX (500 nM; $t_{1/2}$ = 194 s; n = 63 puncta from 3 slices; $p > 0.4$) had no effect on corticostriatal kinetics.

To compare destaining elicited by cortical stimulation to that elicited by striatal stimulation, corticostriatal terminals were loaded with FM1-43 using 10 Hz stimulation over cortical layers 5–6. The electrode was then repositioned over the border of the corpus callosum and striatum. Destaining puncta were visualized with the imaging window positioned over the lateral striatum just medial to the stimulating electrodes. Striatal 10 Hz pulse stimulation resulted in rapid destaining ($t_{1/2}$ = 57 ± 4.6 s; mean ± SEM; n = 140 puncta from 3 slices) similar to values from prior experiments that utilized direct terminal excitation to unload FM1-43 (Betz and Bewick, 1992; Isaacson and Hille, 1997) and greater than that obtained by restimulation of the motor cortex ($t_{1/2}$ = 176 s). These results suggest that direct stimulation of distal axons and/or synaptic terminals results in greater destaining rates than stimulating cell bodies, possibly due to a certain action potential generation/propagation failure rate or voltage-dependent activation of synaptic terminal second messenger systems.

Synaptic Dopamine Regulates the Release of FM1-43 from Corticostriatal Terminals

To determine whether synaptically released dopamine in the striatum modulates presynaptic terminal activity, we examined corticostriatal destaining while releasing endogenous dopamine (Figure 4A). The bulk of studies to date have interpreted presynaptic actions of dopamine following stimulation of corticostriatal fibers en passant by applying current to the corpus callosum. To our knowledge, no one has measured whether current spread might also stimulate dopamine release from striatal terminals, which could occlude observation of genuine effects. Cyclic voltammetry demonstrated that stimulation of the corpus callosum itself elicited dopamine release; for example, in the striatum ~200–300 μm from the corpus callosum, a single pulse 400 μA, 1 ms stimulus evoked a peak concentration of 0.36 ± 0.07 μM (n = 4) dopamine. In contrast, cortical stimulation elicited no dopamine release (Figure 4B) so long as the stimulation electrodes were dorsal to the corpus callosum.

Rodents exposed to behaviorally salient stimuli display a rapid pulsatile elevation of striatal dopamine that reaches 200–500 nM and declines to background in <1 s (Robinson et al., 2001). Striatal stimulation at 0.1 Hz evoked striatal dopamine release in a manner similar to behavioral stimuli associated with activation of reward/expectation pathways, reaching a peak level of ~1–2 μM for the first stimulus and eventually decreasing to a plateau of ~30% of initial concentration (Figures 4C and 4D). At this frequency, striatal stimulation alone had no measurable affect on puncta fluorescence, suggesting negligible interaction on glutamatergic afferents (Figure 2B).

Striatal stimulation inhibited corticostriatal destaining ($t_{1/2}$ = 260 s versus 176 s for control; $p < 0.001$; Figure 5A). The response was sensitive, as the first optical measurement (90% ± 1.6% versus 85% ± 1.4% destaining for controls at 22.5 s; mean ± SEM, $p < 0.02$), during which only two synaptic dopamine release events were evoked, showed a 67% (100-85/100-90) depression of

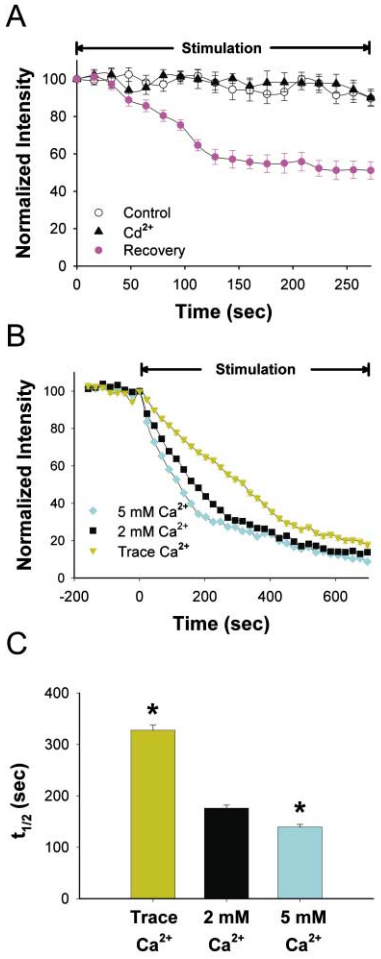

Figure 3. Ca^{2+} Dependence of Corticostriatal Terminal Destaining

(A) Terminal destaining was measured during a control period without cortical stimulation (Control) and during stimulation in 200 μM Cd^{2+}. Destaining with Cd^{2+} was identical to unstimulated controls. After a 15 min washout, stimulation-dependent destaining recovered (n = 74 puncta from 3 slices).

(B) Calcium dependence was demonstrated by destaining slices in control aCSF (2 mM Ca^{2+}, 1.2 mM Mg^{2+}; n = 193 puncta from 8 slices), high Ca^{2+} aCSF (5 mM Ca^{2+}, 1.2 mM Mg^{2+}; n = 199 puncta from 6 slices), and trace calcium aCSF (0 mM Ca^{2+}, 1.2 mM Mg^{2+}; n = 206 puncta from 5 slices).

(C) Distribution of mean $t_{1/2}$ values for the three Ca^{2+} concentrations, mean ± SEM. *$p < 0.001$ compared to control (2 mM Ca^{2+}).

corticostriatal terminal activity by dopamine release. While most terminals showed a slower destaining rate in the presence of dopamine, there was still a small fraction of rapidly destaining puncta (Figure 5B). Histograms of individual terminal destaining times revealed a rightward shift for most terminals exposed to synaptically released dopamine (Figure 5C). When the $t_{1/2}$ of each terminal was displayed in a normal probability plot, in which a straight line signifies a normal distribution, it was apparent that the most rapidly destaining terminals (~15%) were unaffected by dopamine, whereas the majority (~85%) exhibited slower destaining times following dopamine release (Figure 5D).

In order to examine a potential role for a glutamate-evoked feedback pathway on the response to dopamine, we repeated the experiments in the presence of a cocktail of glutamate receptor antagonists. Corticostriatal destaining half-times with simultaneous striatal stimulation (0.1 Hz) in the presence of (*S*)-MCPG (300 μM), NBQX (10 μM), and D-APV (50 μM) were similar to dopamine-exposed sections ($t_{1/2}$ = 246 s versus 260 s, $p > 0.3$). The absence of a measurable effect by glutamate receptor antagonists suggests that, in this preparation, presynaptic responses are independent of postsynaptic feedback mechanisms that rely on glutamate release evoked from the corticostriatal terminals.

Next, we examined if striatal dopamine exerted its influence on corticostriatal terminals through cholinergic, GABAergic, or adenosine interneurons or receptors. Corticostriatal destaining half-times in the presence of the muscarinic receptor antagonist atropine (10 μM; $t_{1/2}$ = 195 s; n = 77 puncta from 3 slices; $p > 0.1$) and the nicotinic receptor antagonist mecamylamine (100 μM; $t_{1/2}$ = 199 s; n = 106 puncta from 3 slices; $p > 0.1$) were similar to controls (176 s). Atropine with striatal stimulation did not affect corticostriatal destaining times ($t_{1/2}$ = 290 s, n = 77 puncta from 3 slices; versus $t_{1/2}$ = 260 s for striatal stimulation alone; $p > 0.2$). Likewise, mecamylamine (100 μM; $t_{1/2}$ = 274 s, n = 106 puncta from 3 slices; $p > 0.9$), the $GABA_B$ antagonist CGP 52432 (10 μM; $t_{1/2}$ = 321 s; n = 129 puncta from 4 slices; $p > 0.05$), or the adenosine A1 antagonist DPCPX (500 nM; $t_{1/2}$ = 306 s; n = 68 puncta from 3 slices; $p > 0.2$) combined with quinpirole (1 μM) did not block the inhibition of destaining measured in sections exposed to quinpirole alone ($t_{1/2}$ = 288 s; n = 77 puncta from 3 slices).

To elevate extracellular dopamine levels in a different manner, we tested the effects of amphetamine, which induces continuous dopamine efflux from nigrostriatal terminals via reverse transport (Jones et al., 1998; Schmitz et al., 2001). Figure 5E shows an example of striatal dopamine efflux in response to amphetamine superfusion (10 μM for 20 min). The maximal level of dopamine reached ~6 μM within 10–20 min. Amphetamine inhibited corticostriatal activity to a similar extent as electrically evoked synaptic dopamine release ($t_{1/2}$ = 266 s; $p = 0.344$), as did the combination of stimulation and amphetamine ($t_{1/2}$ = 270 s versus 176 s for control; $p < 0.001$; Figures 5A, 5C, and 5D).

Corticostriatal Activity Is Regulated by D2 Dopamine Receptors

We used specific dopamine receptor ligands to determine which receptor was responsible for the depression of corticostriatal activity. The D2-like receptor antagonist, sulpiride (10 μM), induced a small but significant enhancement of destaining ($t_{1/2}$ = 150 s versus 176 s for controls; $p < 0.01$; Figures 6A, 6C, and 6D), suggesting a low level of ongoing D2 receptor activity independent of dopamine release. Sulpiride completely blocked the effect of striatal stimulation ($t_{1/2}$ = 170 s versus 269 s for stimulated sections; $p < 0.001$), resulting in destaining curves comparable to controls ($t_{1/2}$ = 176 s; $p > 0.5$; Figures 6A and 6C). Sulpiride at a lower concentration (100 nM) also blocked the effect of dopamine elicited by striatal stimulation ($t_{1/2}$ = 179 s sulpiride-treated sections; n = 67 puncta from 4 slices; versus 191 s for stimulated sections with sulpiride; n = 49 puncta from

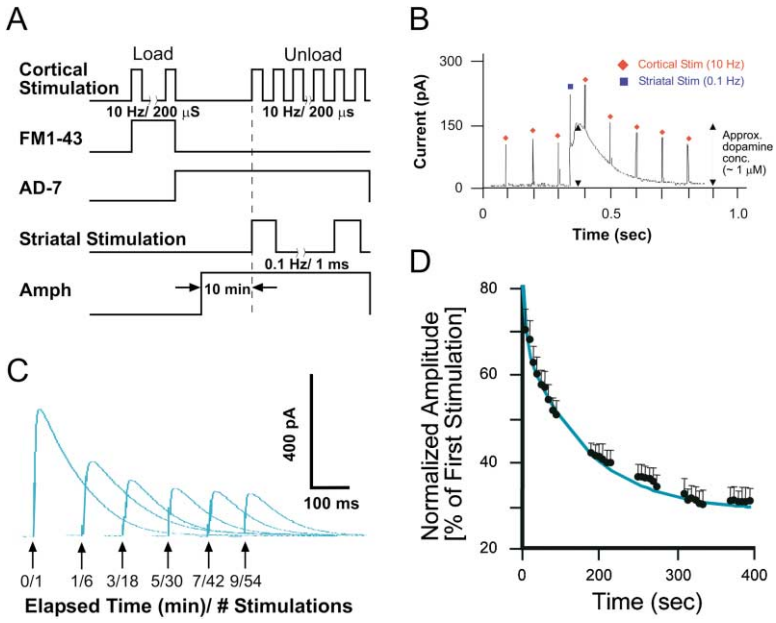

Figure 4. Striatal Stimulation Elicits Dopamine Release

(A) Protocol for loading and unloading corticostriatal terminals with FM1-43 in the presence of synaptic dopamine. Synaptic striatal dopamine release was evoked by either 0.1 Hz stimulation of the motor striatum (1 ms, 400 μA) or by amphetamine (Amph; 10 μM). Amphetamine was superfused for 10 min prior to cortical stimulation.

(B) Amperometric recordings show that striatal stimulation (stimulus artifact marked by a blue square) elicited dopamine release to a maximum concentration of ~1 μM. Concurrent 10 Hz cortical stimulation (stimulus artifacts marked by an orange diamond) failed to elicit dopamine release. The substance released by this protocol has been identified as dopamine by cyclic voltammetry (Schmitz et al., 2001).

(C) Amperometric recordings of evoked dopamine overflow in response to the first stimulation and after 1, 3, 5, and 9 min of a 0.1 Hz stimulation train.

(D) The maximum amplitude of dopamine overflow for the first stimulus, as measured with cyclic voltammetry, was between 1 and 2 μM and decreased to ~30% of initial levels.

4 slices; $p > 0.6$). In contrast, the D1-like receptor antagonist, SCH 23390 (10 μM), had no effect on destaining either in the absence ($t_{1/2} = 177$ s; $p > 0.5$) or presence ($t_{1/2} = 245$ s; $p > 0.1$; Figure 6A) of stimulated synaptic dopamine release. Likewise, a lower concentration of SCH 23390 (20 nM) did not alter destaining rates with ($t_{1/2} = 279$ s; $p > 0.5$) or without ($t_{1/2} = 193$ s; $p > 0.5$) striatal stimulation. The D2-like receptor agonist quinpirole (0.5 μM) inhibited terminal destaining to the same extent as stimulated or amphetamine-induced dopamine release ($t_{1/2} = 247$ s for quinpirole versus 176 s for controls; $p < 0.001$; Figures 6B–6D). The D1-like receptor agonist, SKF 38393, had no effect on terminal activity ($t_{1/2} = 179$ s; $p > 0.5$; Figure 6A).

To confirm the dopamine receptor responsible for the modulation of corticostriatal terminal activity, we examined D2 receptor knockout ($D2^{-/-}$) mice (Jung et al., 1999). Untreated mutants exhibited higher activity than congenic wild-type siblings ($t_{1/2} = 141$ s versus 176 s for $D2^{-/-}$ and wild-type, respectively; $p < 0.001$; Figure 6B), with a distribution of destaining kinetics for individual terminals nearly identical to sulpiride-treated wild-types (Figures 6C and 6D). $D2^{-/-}$ mutants had no response to quinpirole ($t_{1/2} = 143$ s for quinpirole-treated $D2^{-/-}$ mice versus 140 s for $D2^{-/-}$ mice, respectively; $p > 0.5$) or combined amphetamine and striatal stimulation ($t_{1/2} = 145$ s; $p > 0.5$; Figures 6B and 6C).

The Magnitude of Dopamine-Mediated Inhibition Is Determined by the Frequency of Cortical Stimulation

Corticostriatal cell bodies are reported to exhibit oscillations between up and down states at a peak frequency of ~1 Hz and spiking within up states at median intervals of 20–40 Hz (Stern et al., 1997). To observe the effects of a lower and higher frequency of cortical stimulation, we unloaded corticostriatal terminals with bipolar stimulation of the motor cortex at 1, 10, and 20 Hz (Figure 7A). To observe the effects of stimulated dopamine release at these frequencies, we simultaneously stimulated the striatum with 0.1 Hz pulses (Figures 7B–7D). The average half-time of terminal unloading at 1 Hz increased with dopamine stimulation from 342 s to 366 s ($p < 0.001$) with slower destaining of the 20% least active terminals (Figure 7B). At 20 Hz, dopamine inhibited the release of FM1-43 from ~80% of terminals ($t_{1/2} = 155$ s versus 285 s, $p < 0.001$; Figure 7D), similar to values obtained at 10 Hz (Figure 7C), although the extent of dopamine's effect on destaining was greater at 20 Hz than at 10 Hz. Thus, the magnitude of dopamine inhibition becomes progressively greater at higher corticostriatal stimulation frequencies, with a 1.1-fold inhibition for the mean $t_{1/2}$ values at 1 Hz (366/342 s), 1.5-fold inhibition at 10 Hz (260/176 s), and 1.8-fold inhibition at 20 Hz (285/155) ($p < 0.01$ for interaction between dopamine and stimulation frequency, $F = 10.28$, two-way ANOVA).

Finally, to examine possible effects of presynaptic inhibition by D2 receptors on individual MSNs, we conducted whole-cell patch clamp recordings in voltage clamp mode in 10 medium-sized striatal neurons. EPSCs were evoked by stimulating cortical cell bodies at the same position as for the optical experiments, in the absence of NBQX and while blocking $GABA_A$ receptors with bicuculline (5 μM). Two stimulation frequencies were used (1 and 20 Hz). Each frequency was presented 2–3 times to the cell under each condition to obtain an average. Three stimuli were applied at 1 Hz and three at 20 Hz. The first two EPSCs in each sequence were averaged and compared before and after bath application of quinpirole (0.5 μM, $n = 5$ or 1 μM, $n = 5$). The primary and most consistent effect of quinpirole was a reduction in the average peak amplitude of evoked EPSCs at the 20 Hz stimulus (Figure 8A; -100 ± 12 versus -87 ± 12.2 pA, difference of $-15\% \pm 3.4\%$; $p <$

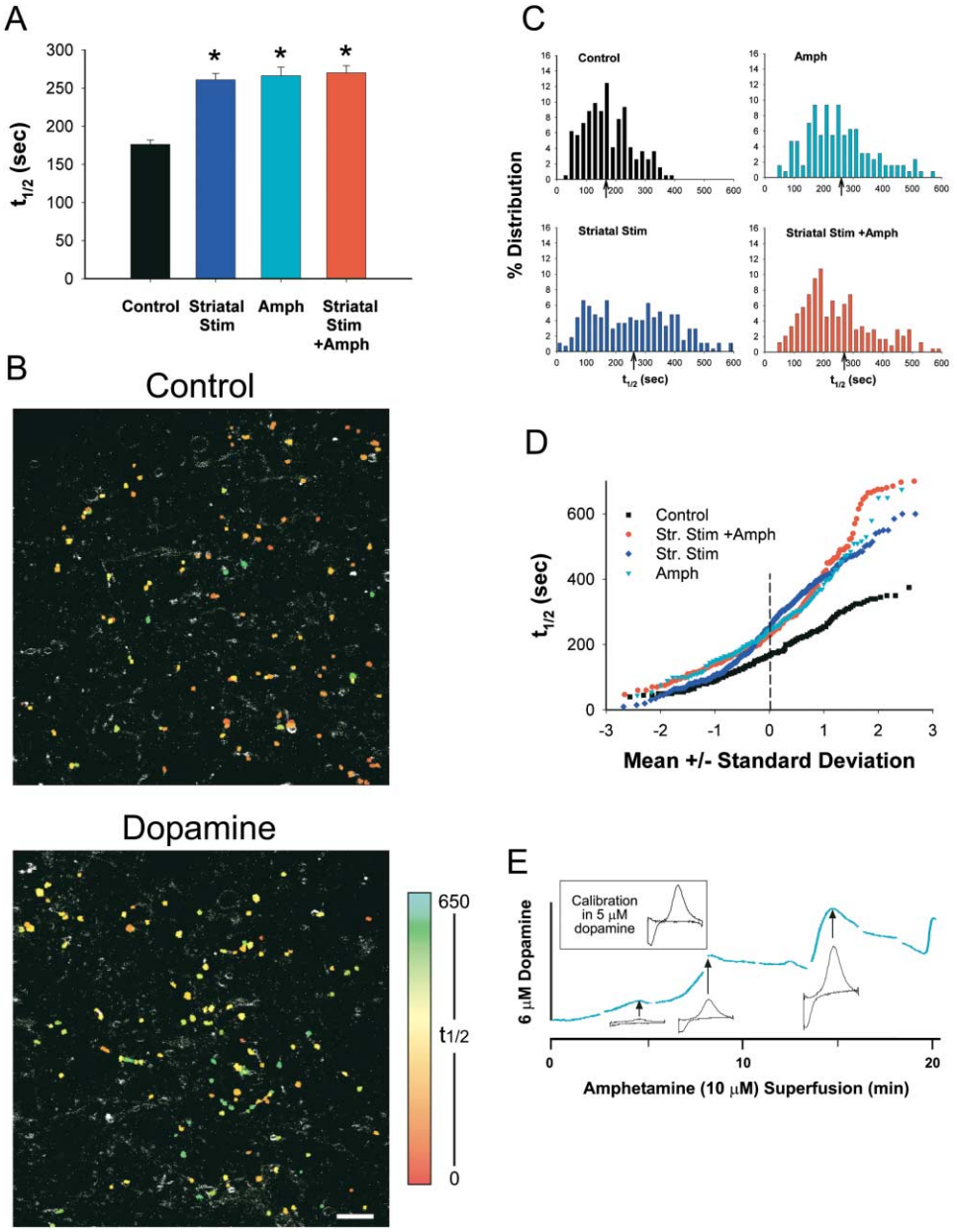

Figure 5. Effects of Striatal Dopamine on Corticostriatal Terminal Kinetics

(A) Distribution of corticostriatal terminal half-times ($t_{1/2}$) during stimulation-evoked striatal dopamine release (Striatal Stim; n = 273 puncta from 7 slices), amphetamine-induced dopamine release (Amph; n = 132 puncta from 6 slices), and combined stimulation-evoked dopamine release and amphetamine (n = 256 puncta from 7 slices), compared to controls with cortical stimulation only (n = 193 puncta from 8 slices). *$p < 0.001$ as compared with the control.

(B) Examples of FM1-43 destaining rates of individual puncta are shown in false color. Note that the preparation exposed to dopamine (bottom; n = 112) has fewer rapidly destaining puncta than the control (top; n = 99). Scale bar equals 10 μm.

(C) Histograms of corticostriatal terminal half-times show a rightward shift (slower destaining times) in terminals exposed to dopamine. Arrows indicate the mean values.

(D) Normal probability plots of $t_{1/2}$ values for each terminal in (A) reveal two populations of terminals that begin to deviate at greater than −1 SD below the mean.

(E) Cyclic voltammetry recording of dopamine efflux evoked by continuous amphetamine superfusion (10 μM) beginning at time t = 0. The background-subtracted voltammograms taken at different time points (arrows) identify dopamine and serve for calibration (inset). A maximum of 6 μM dopamine was reached at ~15 min of amphetamine.

0.001, t = −5.04, df = 9, paired t test). The reduction due to quinpirole at the 1 Hz stimulus was not significant (−89 ± 10.9 versus −73 ± 7.6 pA, difference of −7.6% ± 6.2%; p = 0.218, t = −1.34, df = 8, paired t test). Quinpirole also reduced the frequency of spontaneous synaptic currents in each of five cells examined (from 2.87 ± 0.59 to 1.85 ± 0.43 Hz, n = 5; t = 3.84, df = 4, p = 0.019; Figure 8B). Amplitude-frequency distribution histo-

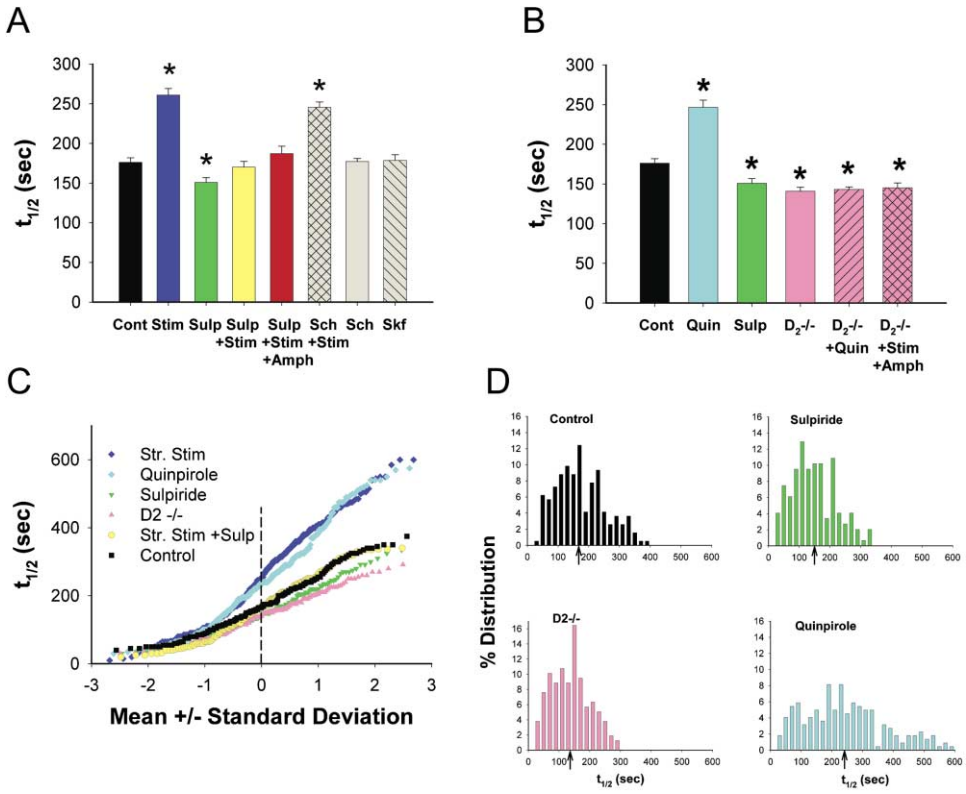

Figure 6. Effects of D2 Receptor Activity on Corticostriatal Terminal Destaining

(A) Corticostriatal terminal destaining half-times ($t_{1/2}$) during stimulated striatal dopamine release (Stim; n = 273 puncta from 7 slices) are compared to controls with no striatal stimulation (Cont; n = 193 puncta from 8 slices). Sulpiride (Sulp; 10 μM; n = 147 puncta from 10 slices) decreases terminal half-times and occludes the effect of striatal stimulation (n = 152 puncta from 7 slices) and the combination of stimulated dopamine release and amphetamine (n = 95 puncta from 5 slices). Additional slices were exposed to the D1-like antagonist SCH 23390 (10 μM) with (Sch + Stim; n = 278 puncta from 9 slices) and without (Sch; n = 386 puncta from 10 slices) stimulated dopamine release. Other nondopamine-exposed slices were treated with the D1-like agonist SKF 38393 (Skf; 10 μM; n = 151 puncta from 6 slices).

(B) Distributions of terminal half-times of destaining in the presence of the D2 receptor agonist quinpirole (Quin; 0.5 μM; n = 221 puncta from 8 slices) and antagonist sulpiride (10 μM; n = 147 puncta from 10 slices) are compared to controls (*D2* wild-type congenic mice; n = 193 puncta from 8 slices, 3 animals). Destaining half-times in $D2^{-/-}$ mice (n = 158 puncta from 9 slices, 4 animals) are similar to those for sulpiride. $D2^{-/-}$ mice exposed to quinpirole (0.5 μM; n = 288 puncta from 7 slices, 3 animals) or to a combination of amphetamine (10 μM) and striatal stimulation (n = 179 puncta from 7 slices, 3 animals) also show low half-times of destaining.

(C) Normal probability plots of $t_{1/2}$ values in (A) and (B). For all affected populations, the distribution reveals at least 2 terminal subpopulations which deviate at values greater than ~1 standard deviation below the mean values.

(D) Histograms show distributions of $t_{1/2}$ values. Arrows indicate mean values that shift to the left (more rapid destaining) with sulpiride and in $D2^{-/-}$ mice and shift to the right with quinpirole. *$p < 0.001$ compared with controls.

grams demonstrated significant reductions in the number of spontaneous EPSCs in the 5–10 and 10–15 pA range ($p < 0.001$; ANOVA followed by Bonferroni t tests; Figure 8C, left histograms) without an effect on relative cumulative amplitude frequencies (Figure 8C, right histograms), suggesting that quinpirole's effect on corticostriatal activity included a presynaptic component.

Discussion

Synaptic arrangements consisting of dendrites with fast-acting glutamatergic or GABAergic inputs and closely neighboring modulatory inputs that activate G protein-coupled receptors are common in the brain. Perhaps the most studied system has been the corticostriatal-mesostriatal synapses on medium spiny neuronal dendrites. The effect of dopamine release on the activity of excitatory corticostriatal inputs is highly controversial (see Introduction). One likely reason underlying the apparently contradictory reports is that previous studies have all been conducted by postsynaptic recording of MSNs, which cannot demonstrate differential responses by subpopulations of corticostriatal terminals. Moreover, many previous studies stimulated corticostriatal fibers in a manner that likely elicited striatal dopamine release, potentially occluding effects of dopamine or dopamine receptor agonists.

We developed an approach to directly measure effects of synaptic dopamine release at presynaptic corticostriatal terminals and have thus identified an example of axo-axonic modulation of presynaptic activity by G protein-coupled receptors in the central nervous system. In addition, our approach evoked synaptic dopamine release and reuptake with kinetics that closely resemble those reported in awake behaving animal presented with behavioral stimuli. As stimulation of cortico-

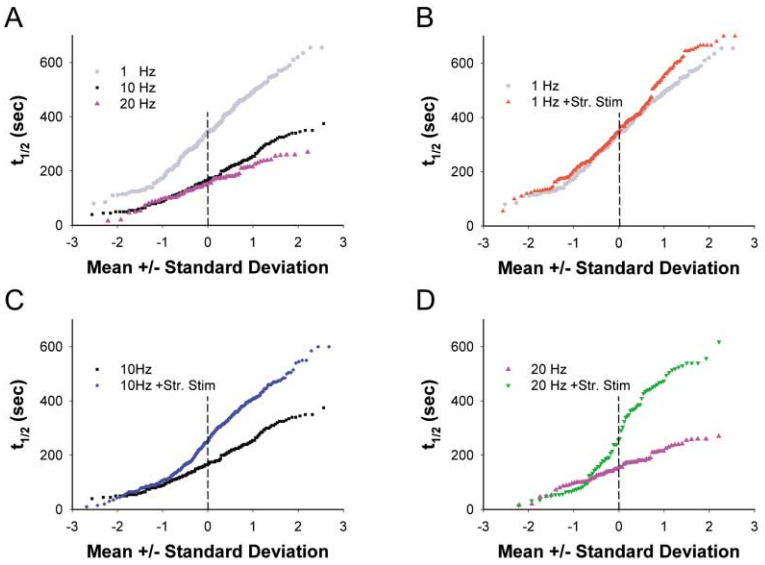

Figure 7. Effects of Corticostriatal Stimulation Frequency and Evoked Dopamine Release on Terminal Destaining

(A) Normal probability plots of $t_{1/2}$ values for each terminal following cortical stimulation at 1, 10, and 20 Hz (1 Hz, n = 172 puncta from 5 slices; 10 Hz, n = 193 puncta from 8 slices; 20 Hz, n = 75 puncta from 3 slices).

(B–D) Normal probability plots at 1, 10, and 20 Hz corticostriatal stimulation frequencies with and without evoked dopamine release by 0.1 Hz striatal stimulation (1 Hz, n = 195 puncta from 4 slices; 10 Hz, n = 273 puncta from 7 slices; 20 Hz, n = 74 puncta from 3 slices).

striatal fibers occurred far from their terminals, while striatal dopamine was released far from cortical cell bodies, and as the effects of dopamine were independent of glutamate blockade, we conclude that the response to dopamine appears to be heterosynaptic, i.e., due to axo-axonal neurotransmission. The electrophysiological data independently confirm that D2 agonists exert a heterosynaptic inhibitory effect on corticostriatal synaptic transmission, as demonstrated by the inhibition of spontaneous synaptic activity by quinpirole. This is consistent with some previously published work in striatal slices, in which spontaneous synaptic activity enhanced by K^+ channel blockers (e.g., 4-aminopyridine) is reduced by acute application of quinpirole in a subset of striatal neurons (Flores-Hernández et al., 1997), while under more chronic conditions, there is evidence that mice lacking D2 receptors have increased spontaneous synaptic activity (Cepeda et al., 2001; Tang et al., 2001). More broadly, our findings complement reports that presynaptic G protein-coupled neurotransmitter receptors including glutamatergic, GABAergic, and cholinergic receptors typically inhibit neurotrans-

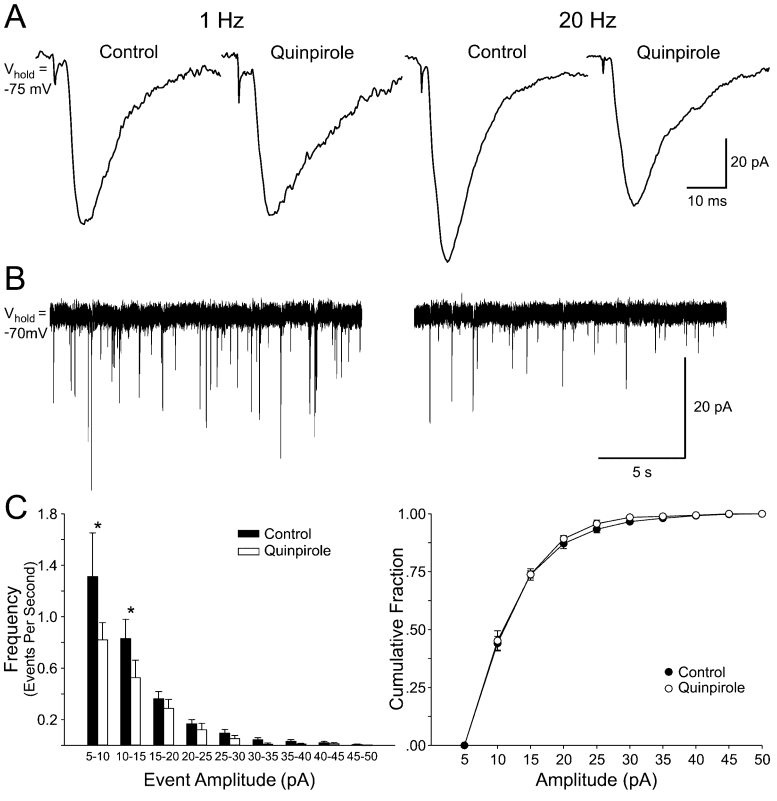

Figure 8. Electrophysiological Effects of Quinpirole

(A) Each trace represents the response average (2–3 stimuli) before (left) and after (right) quinpirole (0.5–1 μM) at two frequencies of stimulation, 1 Hz (left pair of traces) and 20 Hz (right pair of traces). Note the greater reduction in peak amplitude after quinpirole at 20 Hz.

(B) Spontaneous EPSCs in control conditions (left trace) and after 5 min in quinpirole (0.5 μM, right trace).

(C) Left: Average amplitude-frequency histogram of spontaneous EPSCs before and after quinpirole (n = 5 cells). Significant reductions in frequency occurred in the 5–10 and 10–15 pA amplitude bins (asterisks). Right: Cumulative normalized amplitude-frequency histogram in control and quinpirole conditions. The cumulative normalized amplitude-frequency distributions were not altered after quinpirole.

mitter release (Nicoll et al., 1990; Thompson et al., 1993; Zhang and Sulzer, 2003).

By visualizing vesicular release from individual terminals, we found that at each corticostriatal stimulation frequency, the most active terminals appeared selectively resistant to dopamine D2 receptor-dependent inhibition, while the remaining terminals were inhibited. This is similar to a finding from hippocampal autapses, in which the ~16% of boutons with higher release probability were selectively resistant to presynaptic GABAergic inhibition, while ~84% were depressed (Rosenmund et al., 1993). Although the precise mechanism of dopamine's activity-dependent heterosynaptic filtering is unknown, its persistence under glutamate, GABAergic cholinergic, and adenosine receptor blockade, as well as its complete inhibition by a D2 antagonist and lack of response in a D2 knockout mutant, are consistent with activation of presynaptic D2 receptors on corticostriatal axon terminals. Interestingly, stimulation of D2 receptors tilts the balance of synaptic plasticity toward short- and long-term depression, as absence of this DA receptor subtype favors the emergence of long-term potentiation (Calabresi et al., 1997). The presence of presynaptic D2 receptors on corticostriatal axon terminals is supported by some anatomical (Fisher et al., 1994; Hersch et al., 1995; Sesack et al., 1994; Wang and Pickel, 2002) and electrophysiological (Calabresi et al., 1993; Cepeda et al., 2001; Flores-Hernandez et al., 1997; Hsu et al., 1995; O'Donnell and Grace, 1994; Tang et al., 2001; West and Grace, 2002) evidence. Nevertheless, while the evidence indicating involvement of presynaptic D2 receptors is strong, it remains possible that receptors other than or in addition to those on corticostriatal terminals are involved in this form of presynaptic inhibition.

In the FM1-43 destaining experiments, we found that the magnitude of dopamine's inhibitory effect progressively increased at 1, 10, and 20 Hz corticostriatal stimulation frequencies, with dopamine-exposed terminals at higher frequencies showing distributions of terminal activity that were similar to control terminals stimulated at lower frequency. A dependence of D2-mediated inhibition on stimulation frequency was also consistent with whole-cell recordings in which quinpirole exerted more inhibition at 20 Hz than 1 Hz. This stands in contrast to studies of presynaptic GABAergic inhibition, which is greater at lower frequencies (Brager et al., 2003; Isaacson and Hille, 1997). The reasons underlying different frequency-dependent modulatory responses are unclear. One possibility is suggested from our results indicating that corticostriatal activity was profoundly regulated by stimulus frequency, with marked short-term depression at 10 Hz and higher frequencies. Frequency-dependent short-term depression has been suggested to occur when the refilling of synaptic vesicles from a reserve pool to the releasable pool, a Ca^{2+}-dependent step, cannot keep up with enhanced exocytosis and becomes rate limiting (Lin et al., 2001; Neher and Sakaba, 2001). In this case, presynaptic inhibition of the refilling step could provide additional inhibition at higher frequencies. Alternatively, corticostriatal boutons might have a lower intrinsic probability of release at higher frequencies, and as above, this would be consistent with the selective filtering of less active corticostriatal inputs. Further studies are needed to examine these and other possible mechanisms.

Together, the data suggest the hypothesis that in the dynamic and kinetic range of dopamine input associated with salient behavioral stimuli, the most active corticostriatal inputs are selected by filtering out the activity of the less active inputs. While the mechanism of interaction between dopamine and the frequency of corticostriatal stimulation is not understood, we speculate that this effect could indicate how dopamine release associated with salience interacts with a highly activated cortical input during motor learning to reinforce specific subsets of corticostriatal connections. We also found that the effects of amphetamine on corticostriatal terminal activity were nearly identical to those from evoked synaptic dopamine release. Thus, psychostimulant drugs may dissociate the time-coding characteristics of behaviorally relevant activation of dopamine input, leading to aberrant filtering of less active corticostriatal inputs. Such actions may indicate how drugs of abuse reinforce drug-taking behavior, leading to the development of dependence.

Experimental Procedures

FM1-43 Loading and Destaining

We used adult congenic C57BL/6 D2 receptor −/− mice and their wild-type littermates (Jung et al., 1999) anesthetized with ketamine/xylazine. All animal protocols were approved by the IACUC of Columbia University and the University of Washington. Acute 200 μm thick coronal striatal brain slices containing the cortex were cut on a vibratome and allowed to recover for 1 hr in artificial CSF solution (aCSF, in mM: 109 NaCl, 5 KCl, 35 $NaHCO_3$, 1.25 $NaHPO_4$, 1.2 $MgCl_2$, 2 $CaCl_2$, 10 D-Glucose, 20 HEPES acid [pH 7.3–7.4], 295–305 mOs) at room temperature. To prevent a glutamate-mediated retrograde effect on presynaptic terminals, the AMPA/kainate receptor antagonist NBQX (10 μM) was included in the aCSF except where noted. Experiments were performed on the second to fourth frontal slice of caudate putamen [bregma, +1.54 to +0.62 mm]. For each experiment, slices were enclosed in a RC-27L incubation chamber (56 μl/mm; Warner Instruments, Hamden, CT) perfused at 2 ml/min with aCSF at +37°C.

FM1-43 (N-[3-(triethylammonio)propyl]-4-(4-dibutylaminostyryl) pyridinium dibromide; Molecular Probes; 8 μM in aCSF) was loaded into presynaptic terminals by a 10 min train of 200 μs pulses at 10 Hz, 400 μA applied to cortical layers V-VI. To remove dye bound to extracellular tissue, sections were then incubated in ADVASEP-7 (CyDex, Overland Park, KS; 0.1 mM in aCSF; Kay et al., 1999). For stimulation-dependent corticostriatal terminal loading and destaining, and to elicit dopamine release, pulse trains were applied to the cortex or striatum using bipolar twisted tungsten electrodes. Electrical stimulation was provided by a Tektronix R564B wave generator (Tektronics, Gaithersburg, MD) through a stimulation isolator (AMPI, Jerusalem, Israel) and monitored by a S88 storage oscilloscope (Grass-Telefactor, West Warwick, RI).

With the exception of NBQX (AG Scientific, San Diego, CA) and CGP 52432 (Tocris, Ellisville, MO), all drugs were purchased from Sigma (St. Louis, MO): D-APV (D(-)-2-amino-5-phosphonopentanoic acid); (+/−)-quinpirole; atropine; mecamylamine; (S)-MCPG; bicuculline; S(-)-sulpiride; R(+)-SKF 38393; R(+)-SCH 23390; DPCPX; and (+) amphetamine sulfate. Slices were allowed to rest for at least 10 min in the drug to ensure equilibrium.

Imaging and Data Analysis

Striatal terminals were visualized using a Zeiss LSM 510 NLO multiphoton laser scanning confocal microscope with a Titanium-sapphire laser (excitation 855 nm/emission 625 nm) equipped with a 40× 0.8 NA water immersion ultraviolet objective (Zeiss). Images were captured in 8-bit, 123 × 123 μm regions of interest at 512 × 512 pixel resolution and acquired at 22.5 s intervals using Zeiss

LSM 510 software. To compensate for minor z-axis shift, a z-series of seven images, separated by 1 μm in the z-plane, was obtained for each period. Images in each z-series were aligned and condensed with maximum transparency. The time projection was analyzed for changes in puncta fluorescence using Image J (Wayne Rosband, National Institutes of Health, Rockville, MD) or custom-written software in IDL (Research Systems, Boulder, CO) (Zakharenko et al., 2001). The striatal region of interest (ROI) where fluorescent puncta were analyzed was 1.5–2.0 mm distant from the cortical stimulation electrodes. For dopamine stimulation experiments, bipolar electrodes were placed over the motor striatum and visualized on the edge of the ROI. Fluorescent puncta 0.5–1.5 μm in diameter were identified. The criteria for including puncta were (1) spherical shape, (2) fluorescence two standard deviations above the background, and (3) stimulation-dependent destaining. The program aligned puncta in the x, y, and z planes by shifting each image in three dimensions based on the location of the peak of their cross correlograms with the first z-series. Images showing projections of maximal z-axis intensity were made of each stack, and the intensity of FM1-43 fluorescence for each punctum was measured over the time interval. To correct for minor changes in background fluorescence (due to minor tissue bleaching), the background fluorescence of each image (<10%) was subtracted from the fluorescence intensity of individual puncta. The results were then normalized by the maximal fluorescence intensity of that punctum following the FM1-43 loading procedure before unloading. The half-time decay of intensity during destaining ($t_{1/2}$) was determined graphically, in some instances using a 5th degree polynomial smoothing function on SigmaPlot (SPSS, Chicago, IL) software. The fractional release parameter f was calculated from $\ln (F_1/F_2)/\Delta AP$ (Isaacson and Hille, 1997) where ln is the natural logarithm, F_1 and F_2 are the fluorescent intensities at t_1 and t_2, respectively, and ΔAP is the number of action potentials delivered during that period. Unless otherwise stated, statistical analysis was performed using the Mann-Whitney U test.

Amperometry and Cyclic Voltammetry

Cylinder carbon fiber electrodes of 7 μm diameter and 30 to 100 μm length were placed into the dorsal striatum. For cyclic voltammetry, a triangular voltage wave (−400 to +1000 mV at 300 V/s versus Ag/AgCl) was applied to the electrode every 100 ms using a waveform generator (Model 39, Wavetek Ltd., Norwich, UK). Current was recorded with an Axopatch 200B amplifier (Axon Instruments, Foster City, CA), with a low-pass Bessel Filter setting at 10 kHz, digitized at 25 kHz (Instrunet board, GW Instruments, Somerville, MA), and acquired with the Superscope II program (GW Instruments). Background-subtracted cyclic voltammograms served to calibrate electrodes and to identify the released substance. For amperometric recordings, a constant voltage of +400 mV was applied to the electrode.

Postsynaptic Recordings

EPSCs were examined in 15 striatal neurons (from 6 mice, 39–60 days) in brain slices (350 μm thick). Standard techniques were used to prepare slices for electrophysiology (Cepeda et al., 2001). Infrared videomicroscopy coupled with differential interference contrast optics was used to visually identify medium-sized neurons before recording. The external solution consisted of standard artificial cerebrospinal fluid (ACSF) (in mM): NaCl 130, $NaHCO_3$ 26, KCl 3, $MgCl_2$ 2, NaH_2PO_4 1.25, $CaCl_2$ 2, glucose 10 (pH 7.4). Whole-cell patch clamp recordings in voltage-clamp mode were used to examine spontaneous and evoked EPSCs. The patch pipette (3–5 Mohms) contained the following solution (in mM): Cs^+-methanesulfonate to block K^+ currents 130, CsCl 10, NaCl 4, $MgCl_2$ 1, MgATP 5, EGTA 5, HEPES 10, GTP 0.5, phosphocreatine 10, leupeptin 0.1, and 4 QX-314 to block Na^+ channels internally (pH 7.25–7.3, 280–290 mOsm/l). EPSCs were isolated by blocking $GABA_A$ receptors with bicuculline (BIC, 5 μM). The stimulating and recording electrodes were placed in the same locations as described in the FM1-43 experiments and the stimulation electrode was the same as that used in the imaging studies. Stimulation intensity (1.0–2.5 mA, mean 1.5 ± 0.1 mA) was adjusted to 1.5× threshold (EPSC peak amplitude range was −49 to −206 pA, mean ± SE, −91 ± 14 pA). Two stimulation frequencies were used (1 and 20 Hz). Each frequency was presented 2–3 times to the cell under each condition to obtain an average. Three stimuli were applied at 1 Hz and three at 20 Hz. The first 2 EPSCs in each sequence were averaged and compared before and after bath application of quinpirole (0.5 μM, n = 5 or 1 μM, n = 5). Results did not differ between these two concentrations and data were pooled.

Spontaneous postsynaptic inward currents also were recorded in ACSF containing BIC (5 μM). In addition, cells were held at −70 mV to further minimize the contribution of $GABA_A$-mediated events and that of voltage-gated conductances. Spontaneous EPSCs were recorded for 3–5 min. The membrane current was filtered at 1 kHz and digitized at 200 μs using Clampex (gap free mode). Spontaneous synaptic events were analyzed offline using the Mini Analysis Program (Jaejin Software; Leonia, NJ). The threshold amplitude for the detection of an event was adjusted above root mean square noise level (5 pA). EPSC frequency, amplitude of each event, and amplitude-frequency histograms were examined before and after quinpirole. Frequencies were expressed as number of events per second (Hz).

Supplemental Data

We prepared a QuickTime video showing the destaining in Figure 2A, which can be seen at http://www.neuron.org/cgi/content/full/42/4/653/DC1.

Acknowledgments

We thank Drs. Sara Glickstein, Francois Gonon, Richard Palmiter, Dietmar Plenz, Steve Siegelbaum, and Lisa Zimberg for helpful advice. The authors thank the Colleen Giblin Charitable Foundation for Pediatric Neurology and the Vision Research Center, University of Washington. N.S.B. was a Neurological Sciences Academic Development Awardee at Columbia University. Supported by Children's Hospital and Regional Medical Center, Seattle, WA (N.S.B.), the Child Neurology Society (N.S.B.), NINDS NS33538 (M.S.L.), NIMH MH056123 (C.S.), Charles E. Culpeper Biomedical Pilot Initiative from the Rockefeller Brothers Fund (S.S.Z.), NIDA DA07418 (D.S.), NARSAD (D.S.), NSF (D.S.), the Lowenstein Foundation (D.S.), and the Parkinson's Disease Foundation (D.S.).

Received: September 26, 2003
Revised: March 8, 2004
Accepted: April 14, 2004
Published: May 26, 2004

References

Betz, W.J., and Bewick, G.S. (1992). Optical analysis of synaptic vesicle recycling at the frog neuromuscular junction. Science *255*, 200–203.

Brager, D.H., Luther, P.W., Erdelyi, F., Szabo, G., and Alger, B.E. (2003). Regulation of exocytosis from single visualized GABAergic boutons in hippocampal slices. J. Neurosci. *23*, 10475–10486.

Caille, I., Dumartin, B., and Bloch, B. (1996). Ultrastructural localization of D1 dopamine receptor immunoreactivity in rat striatonigral neurons and its relation with dopaminergic innervation. Brain Res. *730*, 17–31.

Calabresi, P., Mercuri, N.B., Sancesario, G., and Bernardi, G. (1993). Electrophysiology of dopamine-denervated striatal neurons. Implications for Parkinson's disease. Brain *116*, 433–452.

Calabresi, P., Saiardi, A., Pisani, A., Baik, J.H., Centonze, D., Mercuri, N.B., Bernardi, G., and Borrelli, E. (1997). Abnormal synaptic plasticity in the striatum of mice lacking dopamine D2 receptors. J. Neurosci. *17*, 4536–4544.

Cepeda, C., Hurst, R.S., Altemus, K.L., Flores-Hernandez, J., Calvert, C.R., Jokel, E.S., Grandy, D.K., Low, M.J., Rubinstein, M., Ariano, M.A., and Levine, M.S. (2001). Facilitated glutamatergic transmission in the striatum of D2 dopamine receptor-deficient mice. J. Neurophysiol. *85*, 659–670.

Fisher, R.S., Levine, M.S., Sibley, D.R., and Ariano, M.A. (1994). D2 dopamine receptor protein location: Golgi impregnation-gold toned and ultrastructural analysis of the rat neostriatum. J. Neurosci. Res. *38*, 551–564.

Flores-Hernandez, J., Galarraga, E., and Bargas, J. (1997). Dopamine selects glutamatergic inputs to neostriatal neurons. Synapse *25*, 185–195.

Garcia-Munoz, M., Young, S.J., and Groves, P.M. (1991). Terminal excitability of the corticostriatal pathway. I. Regulation by dopamine receptor stimulation. Brain Res. *551*, 195–206.

Garris, P.A., Ciolkowski, E.L., Pastore, P., and Wightman, R.M. (1994). Efflux of dopamine from the synaptic cleft in the nucleus accumbens of the rat brain. J. Neurosci. *14*, 6084–6093.

Gonon, F. (1997). Prolonged and extrasynaptic excitatory action of dopamine mediated by D1 receptors in the rat striatum in vivo. J. Neurosci. *17*, 5972–5978.

Graybiel, A.M., Ragsdale, C.W., Jr., Yoneoka, E.S., and Elde, R.P. (1981). An immunohistochemical study of enkephalins and other neuropeptides in the striatum of the cat with evidence that the opiate peptides are arranged to form mosaic patterns in register with the striosomal compartments visible by acetylcholinesterase staining. Neuroscience *6*, 377–397.

Harvey, J., and Lacey, M.G. (1996). Endogenous and exogenous dopamine depress EPSCs in rat nucleus accumbens in vitro via D1 receptors activation. J. Physiol. *492*, 143–154.

Hersch, S.M., Ciliax, B.J., Gutekunst, C.A., Rees, H.D., Heilman, C.J., Yung, K.K., Bolam, J.P., Ince, E., Yi, H., and Levey, A.I. (1995). Electron microscopic analysis of D1 and D2 dopamine receptor proteins in the dorsal striatum and their synaptic relationships with motor corticostriatal afferents. J. Neurosci. *15*, 5222–5237.

Hsu, K.S., Huang, C.C., Yang, C.H., and Gean, P.W. (1995). Presynaptic D2 dopaminergic receptors mediate inhibition of excitatory synaptic transmission in rat neostriatum. Brain Res. *690*, 264–268.

Isaacson, J.S., and Hille, B. (1997). GABA(B)-mediated presynaptic inhibition of excitatory transmission and synaptic vesicle dynamics in cultured hippocampal neurons. Neuron *18*, 143–152.

Jones, S.R., Gainetdinov, R.R., Wightman, R.M., and Caron, M.G. (1998). Mechanisms of amphetamine action revealed in mice lacking the dopamine transporter. J. Neurosci. *18*, 1979–1986.

Jung, M.Y., Skryabin, B.V., Arai, M., Abbondanzo, S., Fu, D., Brosius, J., Robakis, N.K., Polites, H.G., Pintar, J.E., and Schmauss, C. (1999). Potentiation of the D2 mutant motor phenotype in mice lacking dopamine D2 and D3 receptors. Neuroscience *91*, 911–924.

Kay, A.R., Alfonso, A., Alford, S., Cline, H.T., Holgado, A.M., Sakmann, B., Snitsarev, V.A., Stricker, T.P., Takahashi, M., and Wu, L.G. (1999). Imaging synaptic activity in intact brain and slices with FM1-43 in *C. elegans*, lamprey, and rat. Neuron *24*, 809–817.

Levey, A.I., Hersch, S.M., Rye, D.B., Sunahara, R.K., Niznik, H.B., Kitt, C.A., Price, D.L., Maggio, R., Brann, M.R., Ciliax, B.J., et al. (1993). Localization of D1 and D2 dopamine receptors in brain with subtype-specific antibodies. Proc. Natl. Acad. Sci. USA *90*, 8861–8865.

Lin, Y.Q., Graham, K., and Bennett, M.R. (2001). Depression of transmitter release at synapses in the rat superior cervical ganglion: the role of transmitter depletion. Auton. Neurosci. *88*, 16–24.

Maura, G., Giardi, A., and Raiteri, M. (1988). Release-regulating D-2 dopamine receptors are located on striatal glutamatergic nerve terminals. J. Pharmacol. Exp. Ther. *247*, 680–684.

Neher, E., and Sakaba, T. (2001). Estimating transmitter release rates from postsynaptic current fluctuations. J. Neurosci. *21*, 9638–9654.

Nicola, S.M., and Malenka, R.C. (1998). Modulation of synaptic transmission by dopamine and norepinephrine in ventral but not dorsal striatum. J. Neurophysiol. *79*, 1768–1776.

Nicola, S.M., Kombian, S.B., and Malenka, R.C. (1996). Psychostimulants depress excitatory synaptic transmission in the nucleus accumbens via presynaptic D1-like dopamine receptors. J. Neurosci. *16*, 1591–1604.

Nicola, S.M., Surmeier, J., and Malenka, R.C. (2000). Dopaminergic modulation of neuronal excitability in the striatum and nucleus accumbens. Annu. Rev. Neurosci. *23*, 185–215.

Nicoll, R.A., Malenka, R.C., and Kauer, J.A. (1990). Functional comparison of neurotransmitter receptor subtypes in mammalian central nervous system. Physiol. Rev. *70*, 513–551.

O'Donnell, P., and Grace, A.A. (1994). Tonic D2-mediated attenuation of cortical excitation in nucleus accumbens neurons recorded in vitro. Brain Res. *634*, 105–112.

Robinson, D.L., Phillips, P.E., Budygin, E.A., Trafton, B.J., Garris, P.A., and Wightman, R.M. (2001). Sub-second changes in accumbal dopamine during sexual behavior in male rats. Neuroreport *12*, 2549–2552.

Rosenmund, C., Clements, J.D., and Westbrook, G.L. (1993). Nonuniform probability of glutamate release at a hippocampal synapse. Science *262*, 754–757.

Schmitz, Y., Lee, C.J., Schmauss, C., Gonon, F., and Sulzer, D. (2001). Amphetamine distorts synaptic dopamine overflow: effects on D2 autoreceptors, transporters, and synaptic vesicle stores. J. Neurosci. *21*, 5916–5924.

Sesack, S.R., Aoki, C., and Pickel, V.M. (1994). Ultrastructural localization of D2 receptor-like immunoreactivity in midbrain dopamine neurons and their striatal targets. J. Neurosci. *14*, 88–106.

Stern, E.A., Kincaid, A.E., and Wilson, C.J. (1997). Spontaneous subthreshold membrane potential fluctuations and action potential variability of rat corticostriatal and striatal neurons in vivo. J. Neurophysiol. *77*, 1697–1715.

Tang, K., Low, M.J., Grandy, D.K., and Lovinger, D.M. (2001). Dopamine-dependent synaptic plasticity in striatum during in vivo development. Proc. Natl. Acad. Sci. USA *98*, 1255–1260.

Thompson, S.M., Capogna, M., and Scanziani, M. (1993). Presynaptic inhibition in the hippocampus. Trends Neurosci. *16*, 222–227.

Wang, H., and Pickel, V.M. (2002). Dopamine D2 receptors are present in prefrontal cortical afferents and their targets in patches of the rat caudate-putamen nucleus. J. Comp. Neurol. *442*, 392–404.

West, A.R., and Grace, A.A. (2002). Opposite influences of endogenous dopamine D1 and D2 receptor activation on activity states and electrophysiological properties of striatal neurons: studies combining in vivo intracellular recordings and reverse microdialysis. J. Neurosci. *22*, 294–304.

Wilson, C.J. (1987). Morphology and synaptic connections of crossed corticostriatal neurons in the rat. J. Comp. Neurol. *263*, 567–580.

Zakharenko, S.S., Zablow, L., and Siegelbaum, S.A. (2001). Visualization of changes in presynaptic function during long-term synaptic plasticity. Nat. Neurosci. *4*, 711–717.

Zhang, H., and Sulzer, D. (2003). Glutamate spillover in the striatum depresses dopaminergic transmission by activating group I metabotropic glutamate receptors. J. Neurosci. *23*, 10585–10592.